Available online at www.sciencedirect.com
SCIENCE DIRECT®
Journal of Molecular Catalysis A: Chemical 222 (2004) 189–198
JOURNAL OF MOLECULAR CATALYSIS A: CHEMICAL
www.elsevier.com/locate/molcata

Screening of Pd and Ni supported on sol–gel derived oxides for dichloromethane hydrodechlorination

Beatriz Aristizábal[a], Carlos Andrés González[a], Izaskun Barrio[b], Mario Montes[b], Consuelo Montes de Correa[a,*]

[a] *Chemical Engineering Department, Universidad de Antioquia, calle 67 No. 53-108, A.A. 1226, Medellín, Colombia*
[b] *Applied Chemistry Department, Universidad del País Vasco/Euskal Herriko Unibertsitatea, P° Manuel de Lardizábal, 3E-20018 San Sebastián, España*

Received 23 July 2003; received in revised form 31 July 2004; accepted 4 August 2004
Available online 12 September 2004

Abstract

Several alumina, titania, zirconia and silica xerogels modified with approximately 0.05 wt.% Pd or 0.05 wt.% Ni were synthesized by cogellation and conventional impregnation method using Pd and Ni acetylacetonate as metal precursors. Thermolysis of supported complexes was conducted in static air at 300 and 350 °C for Pd and Ni loaded samples, respectively. The resulting catalysts were characterized by XRD, XRF, BET, TPR, and tested in the vapor phase hydrodechlorination of dichloromethane (DCM) with molecular hydrogen. Prior to reaction, catalysts were reduced at 300 °C in 5% H_2/He. The synthetic mixture consisted of 1200 ppm CH_2Cl_2, 1.2% H_2 and balance He at a space velocity of 0.005 g min ml^{-1}. Palladium supported catalysts were more active than those containing nickel, i.e. DCM conversions at 200 °C over Pd(I)–Al_2O_3 almost doubled those obtained over Ni(I)–Al_2O_3 and no intermediate reaction products were observed over Pd supported catalysts whereas CH_3Cl was formed over nickel catalysts. Comparison of the specific activities of selected catalysts expressed as TOF, indicate that the observed differences in activity are related to the nature of the support and the accessibility of the metal function to the fluid phase, even though textural properties also appear to play a role. The most active catalyst, palladium impregnated on sol–gel titania (Pd(I)–TiO_2) had an initial specific activity of 0.36 s^{-1} but, it strongly deactivated after a 48 h exposure to 1200 ppm DCM or by thermolysis of the Pd precursor in static air at 600 °C. Although palladium impregnated in sol–gel alumina exhibited lower activity it was much more stable than Pd(I)–TiO_2.

Keywords: Dichloromethane; Sol–gel catalysts; Pd supported catalysts; Ni supported catalysts; Catalytic hydrodechlorination; Catalyst deactivation

1. Introduction

Chlorinated volatile organic compounds (ClVOCs) play an important role in the chemical industry both as reactants and solvents. The increasing amounts of ClVOCs released into the environment have increased the demand for finding effective methods of their disposal and destruction [1]. The emission of chlorinated compounds to the atmosphere contributes to ozone depletion, smog formation and global warming. Besides, ClVOCs have suspected toxicity and carcinogenic properties [2]. Catalytic hydrodechlorination of ClVOCs could be a safe alternative for the treatment of these wastes since ClVOCs are transformed into harmless non-chlorinated compounds and hydrogen chloride at relatively mild reaction conditions [3–5]. The resulting VOCs products can be recovered or burned, and hydrogen chloride can be separated by alkaline washing. Furthermore, the production of harmful products: phosgene, Cl_2 or fragments of ClVOCs, are minimized [6]. In this sense, catalytic hydrodechlorination has potential economic and environmental advantages over thermal incineration and catalytic oxidation.

Catalytic hydrodechlorination of chlorinated aromatics and chlorinated olefins have been more studied than cloroalkane hydrodechlorination. Hagh and Allen com-

* Corresponding author. Tel.: +57 42105537; fax: +57 42638282.
E-mail address: cmontes@quimbaya.udea.edu.co (C. Montes de Correa).

1381-1169/$ – see front matter © 2004 Elsevier B.V. All rights reserved.
doi:10.1016/j.molcata.2004.08.007

pared Pd and hydrotreatment (Ni, Mo) catalysts for the hydrodechlorination of chloro- and dichlorobenzene [7]. Though the activity of both catalysts was similar for dichlorobenzene hydrodechlorination, the selectivity to chlorobenzene was higher over Pd than over Ni, Mo. Supported noble metals especially Pd, Pt and Rh, have been found active at lower temperatures and pressures than hydrotreatment catalysts for hydrodechlorination of most aliphatic ClVOCs [8]. Among precious metals, systems containing Pd are the most active. Although Ni supported catalysts have proved useful in hydrodehalogenation processes their hydrodechlorination ability is rather limited and they are easily poisoned by HCl produced during reaction. Alumina supported Pd catalysts show better performance than those supported on carbon [8–10]. A disadvantage of the alumina support in the hydrodechlorination of ClVOCs is its low resistance against hydrogen chloride. Surface area decrease and increased surface acidity due to the formation of Al halides which would intensify the trend to coke deposition has been of major concern [11]. Other alternative supports as AlF_3, MgO, ZrO_2 or modified zeolites have been shown to be unstable or exhibit poor performance [12,13]. Therefore, the selection of an appropriate support is an important issue in the development of hydrodechlorination catalysts.

Lately, the sol–gel process has been used to prepare supported metal catalysts and catalyst supports with high thermal stability, resistance to deactivation and flexibility to control catalyst properties such as particle size, surface area and pore size distribution. Numerous authors have shown the ability to disperse catalytic metals on gels whose texture is finely controlled by the sol gel route [14]. When the metal of interest is introduced into the initial solution in the form of a salt (cogellation), it can be incorporated into the framework or partially buried at the surface of the support. In impregnated samples the metal is spread over the carrier surface and is more easily accessible to reactant molecules [15]. In this study we synthesized alumina, titania, zirconia and silica xerogels modified with Pd or Ni by cogellation and conventional impregnation method using Pd or Ni acetylacetonate as metal precursors. The nature of supported Pd or Ni species generated after pretreatment of the acetylacetonate (acac) precursors was investigated. The resulting catalysts were tested in the hydrodechlorination of dichloromethane (DCM). This halomethane was chosen as a model compound since it is the less reactive low molecular weight chlorinated hydrocarbon [16].

2. Experimental

2.1. Catalyst preparation

Catalysts were prepared by modifications of previously reported methods [17–20]. Cogelled alumina supported catalysts containing Pd or Ni were prepared by adding 5 g of aluminum isopropoxide (AIP; Aldrich) to 2.56 g hexilenglicol (HG; Aldrich) and the mixture stirred at 120 °C for 3 h under reflux. About 0.02 g of palladium or 0.03 g of nickel acetylacetonate (Merck, Aldrich) dissolved in acetone was then added and stirred for 5 h. After lowering the temperature to 100 °C, 4.1 ml of water was added dropwise and the system stirred during 4 h. The solvent from gels was removed in a rotavap at 50 °C for 2 h. The solid materials were dried at 100 °C for 1 h, and calcined at 700 °C for 1 h. Catalysts are denoted as Pd(C)–Al_2O_3 and Ni(C)–Al_2O_3.

In the preparation of cogelled silica supported Pd or Ni catalysts, 10 ml of tetraethyl orthosilicate (TEOS; Sigma) and 6.8 ml of ethanol were mixed with 0.04 g palladium or 0.06 g of nickel acetylacetonate (Merck, Aldrich) dissolved in acetone. Then 6.37 ml of water and NH_4OH (pH = 9) was added and the solution stirred at 45 °C for 24 h. Afterwards, the temperature was raised to 80 °C and the gel maintained at this temperature for 1 h. The solvent was removed from gels in a rotavap at 70 °C for 2 h. Solids were dried at 100 °C for 1 h and calcined at 450 °C during 4 h. Catalysts are coded as Pd(C)–SiO_2, Ni(C)–SiO_2.

Cogelled titania supported Pd or Ni catalysts were synthesized by mixing 8 ml titanium isopropoxide (TIP; Acros) and 19.2 ml isopropanol (IP, Merck) at 50 °C. Then, 0.03 g of palladium or 0.05 g nickel acetylacetonate (Merck, Aldrich) dissolved in acetone was added. After adjusting the pH to 9 with NH_4OH (Merck), 11.5 ml deionized water was added dropwise. The gel was stirred under reflux for 23 h at 50 °C. Finally, the temperature was raised to 70 °C and the system stirred at this temperature during 6 h. The solvent was removed from gels in a rotavap at 70 °C for 2 h. Solids were dried at 100 °C for 1 h and calcined at 600 °C during 4 h. Catalysts are denoted as Pd(C)–TiO_2 and Ni(C)–TiO_2.

Zirconia supported Pd or Ni catalysts obtained by cogellation were prepared as follows: 3.2 g of zirconium isopropoxide (ZI, Alfa Aesar) was added to a solution of 10.32 ml of dry isopropanol (IP, Aldrich) and 0.26 ml of HNO_3 (70 wt.%, J.T. Baker). Then, 0.015 g of palladium or 0.024 g nickel acetylacetonate (Merck, Aldrich) dissolved in acetone was added. After stirring for 10 min, a solution of 5.16 ml of isopropanol (Merck) and 0.5 ml deionized water was added at once and the mixture stirred for 2 h at room temperature. The solvent was then removed from the gels at 80 °C for about 2 h in a rotavap and the resulting solids dried at 100° C for 12 h and calcined at 600 °C during 4 h. Catalysts are denoted as Pd(C)–ZrO_2 and Ni(C)–ZrO_2.

Pd and nickel contents of the above catalysts as determined by X-ray fluorescence (XRF) were about 0.6 wt.% (±0.1%). Unmodified supports: alumina, silica, titania and zirconia xerogels were synthesized following the above procedures but, without the addition of the precursor salts. Pd or Ni impregnated on the xerogel oxide supports were prepared by conventional incipient wetness impregnation using acetone solutions of palladium or nickel acetylacetonate (Aldrich) to obtain 0.5 wt.% Pd or 0.5 wt.% Ni on the xerogel oxide supports and calcining the resulting materials at 300 and 350 °C, respectively, during 1 h. Catalysts are coded as Pd(I)-oxide and

Ni(I)-oxide depending on the type of support used. For comparison purposes 0.5 wt.% Pd was also impregnated on commercial alumina (Alpha Aesar 80–120 m^2/g). It was coded Pd(I)–Al_2O_3 (comm.).

2.2. Catalyst characterization

X-ray diffraction (XRD) studies were carried out on a Philips PW 1710 X-ray diffractometer with Cu Kα radiation (=1.5406 Å) and Ni filter. The X-ray tube was operated at 30 kV and 20 mA. Samples were scanned from 2θ = 5°–85° and the X-ray diffraction line positions were determined with a step size of 0.05° and a counting time of 2.5 s per step. The surface area and pore volume of catalysts were determined by N_2 adsorption–desorption at −195 °C in a Micromeritics ASAP 2000 equipment. Samples were previously evacuated overnight at 450 °C under high vacuum. The adsorption data were treated with the full BET equation. N_2 adsorption–desorption experiments were repeated twice and the values of BET surface areas were reproducible within ±5%. The pore size distributions were calculated applying the Barret–Joyner–Halenda (BJH) method to the desorption branches of the isotherms [21]. The assessments of microporosity were made from *t*-plot constructions [22].

Chlorine content of selected samples was determined by X-ray fluorescence (XRF) in a Siemens SRS 3000 sequential spectrophotometer with a rhodium tube as the source of radiation. Palladium dispersions and temperature-programmed reduction (TPR) experiments were carried out using a Thermoquest TPD/R/O 1100 instrument. To measure palladium dispersions by chemisorption of H_2 at 80 °C, the catalysts were first reduced in flowing 5% H_2/Ar heating from room temperature to 300° C at a rate of 2 °C/min and then maintained at this temperature for 2 h. After subsequent evacuation at 300 °C the samples were cooled down to 80 °C under Ar and subjected to H_2 chemisorption (5% H_2/Ar) using a pulse titration procedure. Prior to TPR experiments, the samples were first treated at 120 °C in flowing Ar. Afterwards, they were cooled down to 50 °C in flowing Ar. The reduction was conducted from 50 to 700 °C at a linear ramp of 10 °C/min in a 5% H_2/Ar stream. The apparatus was equipped with TCD and MS detectors and with a drier to remove water from the reduction process. Chemisorption and TPR experiments were repeated up to three times and the hydrogen uptake values were reproducible to within ±5%.

2.3. Catalytic tests

Catalytic experiments were performed in a fixed bed pyrex tubular reactor at atmospheric pressure. Prior to each reaction the catalyst was pretreated in flowing 5% H_2 while being heated at a rate of 2 °C/min to 300 °C and then held at this temperature during 1 h. For a typical reaction, a catalyst weight of 100 mg (particle sizes in the range 250–425 μm) and a total flow of 20 ml/min of a gas stream containing 1200 ppm CH_2Cl_2, 1.2% H_2 and He (balance) were used. The space velocity was 0.005 g min ml^{-1}. Catalysts were stabilized in the reaction mixture at room temperature. After getting stable DCM concentrations (1–3 h), the reaction temperature was increased up to 200 °C and the reaction products monitored by GC-ECD at this temperature; reactor temperature was constant to within ±1 °C. Conversions were obtained from the disappearance of DCM. Each catalytic run was repeated up to three times using fresh samples from the same batch of catalyst and results were reproducible to within ±8%.

During catalytic runs, DCM concentrations varied significantly so the experimental reactor was considered to be an integral reactor. Recently Ordoñez and coworkers [23] found that the kinetics of single organochlorinated compounds over a commercial Pd/Al_2O_3 catalyst can be fitted to a pseudo-first order equation with a reasonable accuracy. Although reaction rate depends on catalyst type, we assumed a first-order rate expression as a first approximation to compare the activity of the synthesized materials and used integral analysis to obtain initial reaction rates [24].

3. Results and discussion

3.1. X-ray diffraction

Fig. 1 shows the X-ray diffraction patterns (XRD) of the unmodified xerogel supports used in this work: Al_2O_3, SiO_2, TiO_2 and ZrO_2, respectively. Trace (a) shows the crystallographic phase characterized by peaks at 2θ = 37.44°, 42.66°, 67.25° corresponding to γ-alumina [25]. Trace (b) shows a broad peak at 2θ = 24° which is characteristic of amorphous silica. Anatase is the only phase obtained in titania supported catalysts (see trace (c)) exhibiting high intensity peaks at 2θ = 25.19°, 37.69° and 47.62° [26]. A mixture of about 63% tetragonal and 37% monoclinic phases was observed for the zirconia support as shown in trace (d) [27]. No additional phases from palladium or nickel oxides were observed in the XRD patterns of the Pd or Ni supported catalysts [28] suggesting that the metal loading was quite low for the sensitivity limits of this technique.

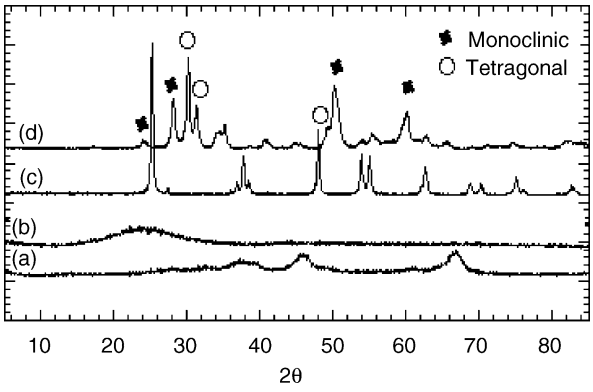

Fig. 1. X-ray diffraction patterns of the unmodified xerogel supports: (a) γ-alumina; (b) silica; (c) titania; (d) zirconia.

Table 1
BET surface area, pore volume, and average pore diameter of cogelled and impregnated Ni and Pd xerogel oxides

Catalyst	BET surface area (m^2/g)	Pore volume (cm^3/g)	Pore diameter (Å)	Micropore area (m^2/g)
Al_2O_3	320	1.16	150	40
Pd(C)–Al_2O_3	367	0.80	65–140	29
Ni(C)–Al_2O_3	369	1.15	95	40
Pd(I)–Al_2O_3	335	0.87	100	24
Ni(I)–Al_2O_3	213	0.57	100	8.1
Pd(I)–Al_2O_3 (commercial)	77	0.42	450	7.6
Ni(I)–Al_2O_3 (commercial)	82	0.40	350	8.1
SiO_2	496	1.0	400	105
Pd(C)–SiO_2	297	0.30	40	57
Ni(C)–SiO_2	249	0.55	400–500	66
Pd(I)–SiO_2	505	0.97	350	101
Ni(I)–SiO_2	500	1.1	600–800	92
TiO_2	30	0.17	150–1100	–
Pd(C)–TiO_2	9	0.03	90–900	1.39
Ni(C)–TiO_2	48	0.18	85–1100	0.27
Pd(I)–TiO_2	33	0.12	80–1100	–
Ni(I)–TiO_2	33	0.12	75–1100	–
ZrO_2	33	0.06	40	1.25
Pd(C)–ZrO_2	52	0.23	30–140	7.3
Ni(C)–ZrO_2	44	0.17	35–650	0.74
Pd(I)–ZrO_2	35	0.075	40–70	0.73
Ni(I)–ZrO_2	23	0.06	50	0.56

3.2. BET surface area and pore size distribution

Table 1 compiles the results of BET surface area, pore volume, and average pore diameter of cogelled and impregnated Ni and Pd xerogel oxides. Alumina based xerogel catalysts exhibited high surface areas. For comparison Pd and Ni were also impregnated in commercial alumina samples (Alpha Aesar 80–120 m^2/g). The surface areas of xerogel alumina supported catalysts are larger than those supported on commercial Al_2O_3. The latter contain larger particles and less microporosity than xerogel alumina supported catalysts. No significant differences were found in the texture of cogelled and impregnated Pd or Ni alumina supported catalysts. The nitrogen adsorption isotherms for the alumina supported materials (not shown) correspond to type IV according to the IUPAC classification and are typical of mesoporous solids. Desorption isotherms for the alumina supported catalysts (not shown) exhibit hysteresis of the Type H1 which is the characteristic of solids consisting of spheroidal particles of uniform size and shape [29]. The addition of Pd or Ni did not significantly change the superficial area or the isotherm type and shape but, decreased the pore diameter. Microporosity was confirmed in xerogel alumina supported catalysts as inferred from Table 1 and from the so-called *t*-plot in which the straight line does not pass through the origin of axes. In all cases the *c* constant from the BET equation is 120–150 confirming that the BET model is in the optimal range $50 < c < 200$.

Silica, and titania xerogel supported catalysts exhibited type II isotherms observed for adsorbents containing macropores. Pd or Ni supported on xerogel titania showed pore size distribution in the mesopore range but, microporosity as well as mesoporosity was observed in Pd or Ni supported on xerogel SiO_2. Most xerogel silica and titania supported samples presented H3 or H4 type hysteresis usually found on solids consisting of aggregates or agglomerates of particles forming slit shaped pores (plates or edged particles like cubes), with nonuniform or uniform size and/or shape [29]. Pd(C)–TiO_2, Ni(I)–SiO_2 and Ni(C)–SiO_2 samples showed a reduced hysteresis loop. This is the case of blind cylindrical, cone-shaped and wedge-shaped pores [29]. Ni(C)–ZrO_2 exhibited isotherm type II, and bimodal pore size distribution exhibiting pores in the meso- and macro-pore range and low microporosity. Pd(I)–ZrO_2 exhibited type IV isotherms. Cogelled Ni or Pd zirconia catalyst exhibited type H3 hysteresis while impregnated ones showed H4 type hysteresis.

3.3. Hydrodechlorination reactions

Fig. 2(a) shows DCM conversion as a function of H_2/DCM ratio over Pd and Ni xerogel alumina supported catalysts at 200° C. The conversion profile of 0.5% Pd impregnated on commercial alumina (Pd(I)–Al_2O_3 (comm.)), is also shown in Fig. 2(a). DCM conversion slightly increases with H_2/DCM ratio on Pd loaded catalysts while it is rather constant over Ni supported alumina catalysts. Ni loaded catalysts and Pd cogelled (Pd(C)–Al_2O_3) samples were much less active than Pd impregnated samples (Pd(I)–Al_2O_3). At H_2/DCM ratios lower than 10 the activity of Pd(I)–Al_2O_3 (comm.) is higher than Pd(I)–Al_2O_3 but, they are close to each other at H_2/DCM = 10. Therefore, this ratio was chosen for further experiments. The temperature profiles of DCM hy-

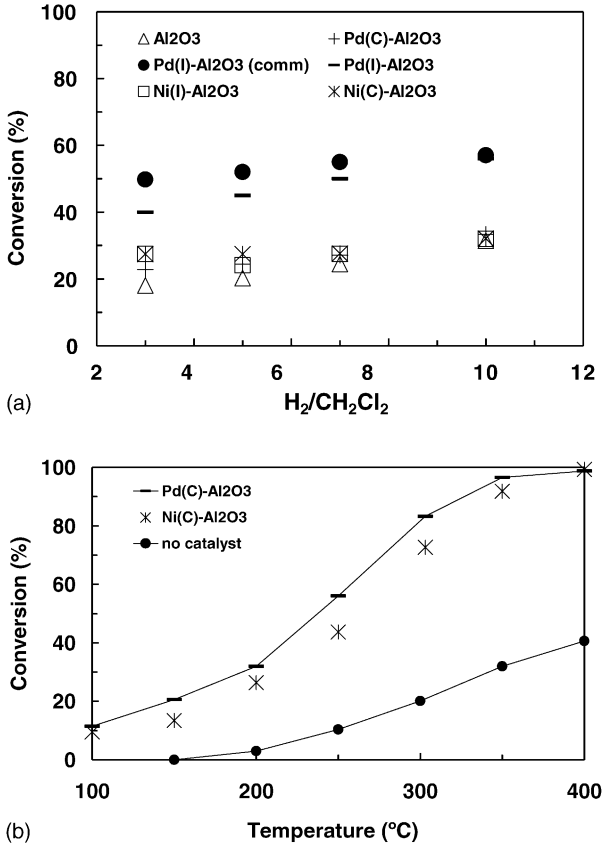

Fig. 2. (a) DCM conversion as a function of H_2/DCM ratio over Pd and Ni xerogel alumina supported catalysts at 200 °C; (b) temperature profiles of DCM hydrodechlorination over Pd(C)–Al_2O_3, Ni(C)–Al_2O_3 and of the homogeneous reaction at H_2/DCM = 10.

drodechlorination at H_2/DCM = 10 over Pd(C)–Al_2O_3 and Ni(C)–Al_2O_3, as well as, that of the homogeneous reaction are compared in Fig. 2(b). It can be observed that a catalyst is required for DCM hydrodechlorination and enables comparison of the metal character on DCM conversion. Pd loaded catalysts appear to be more active than those containing Ni. Formation of other organochlorides was not observed on Pd based catalysts. In contrast, selectivity towards CH_3Cl slightly increased over Ni supported xerogel alumina catalysts. The low selectivity of Ni catalysts may be explained by the high chlorine content on the Ni surface, found by others [30]. In contrast, a PdC_x solid solution has been detected during CH_2Cl_2 hydrodechlorination over a Pd/Al_2O_3 catalyst [31] suggesting that the mildly carbided palladium surface binds intermediate species less strongly, resulting in their more facile hydrogenative desorption [31].

Initial reaction rates (200 °C, H_2/DCM = 10) of Pd and Ni supported on xerogel alumina, silica, titania and zirconia are compared in Fig. 3. Among the catalysts tested Pd(I)–TiO_2 shows the highest activity. The initial DCM reaction rate over impregnated xerogel titania and alumina supported catalysts appears to be a clear function of the type of metal loaded. Ni(I)–Al_2O_3 and Ni(I)–TiO_2 catalysts exhibited much less activity for DCM hydrodechlorination at 200 °C than Pd(I)–Al_2O_3 and Pd(I)–TiO_2, respectively. The difference in activity for cogelled xerogel alumina supported catalysts, Pd(C)–Al_2O_3 and Ni(C)–Al_2O_3, is less significant indicating that in cogelled catalysts the metal function may be inaccessible or difficult to reach by the reactant stream. DCM activity at 200 °C over Pd impregnated catalysts varies in the following order: Pd(I)–TiO_2 > Pd(I)–Al_2O_3 > Pd(I)–ZrO_2 > Pd(I)–SiO_2 while on cogelled ones, Pd(C)–ZrO_2 ∼ Pd(C)–TiO_2 > Pd(C)–SiO_2 ∼ Pd(C)–Al_2O_3. These results are in agreement with those of López et al. [32] who reported that in cogelled ruthenium catalysts a large amount of metal atoms rests in the bulk of the carrier leading to low turnover rates for several reactions.

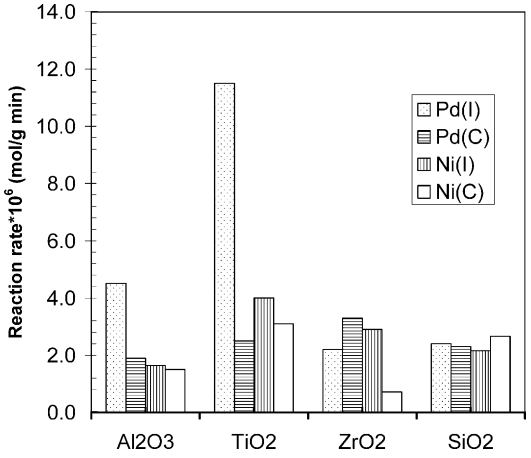

Fig. 3. Initial DCM reaction rates at 200 °C over Pd or Ni loaded on different xerogel supports. H_2/DCM ratio of 10.

Fig. 4 compares the effect of exposing selected catalyst samples to the reaction mixture during 1–3 h or 48 h before DCM hydrodechlorination. Interestingly, Fig. 4 shows that the reaction rate at which DCM disappears over cogelled alumina supported catalysts increased after 48 h pretreatment with DCM. This observation, combined with further evidence presented in the literature [33], leads us to suggest that chloride ions in the alumina support induce agglomeration of Pd clusters which may migrate to the support surface and become more accessible to reactants. As shown in Fig. 4, the activity of Pd(I)–TiO_2 dramatically decreased when exposed 48 h to 1200 ppm DCM before reaction with hydrogen. The decrease observed on Pd(I)–Al_2O_3 or Ni(I)–Al_2O_3 under similar conditions was much lower than on Pd(I)–TiO_2. However, durability tests in the present study indicate that DCM hydrodechlorination is more stable over Pd(I)–Al_2O_3 than over Ni(I)–Al_2O_3, i.e. DCM conversion over Pd(I)–Al_2O_3 was constant at about 44% at 200 °C during 48 h while a conversion decrease from 40% to about 20% after 36 h was observed over Ni(I)–Al_2O_3 under the same conditions. Table 2 shows chloride contents of selected samples as determined by XRF. Table 2 suggests that Pd is less prone to deactivation by chlorine than Ni. Choi and Lee reported that adsorbed HCl modified the crystal structure of metallic Ni to $NiCl_2$ leading to irreversible catalyst deactivation and metal

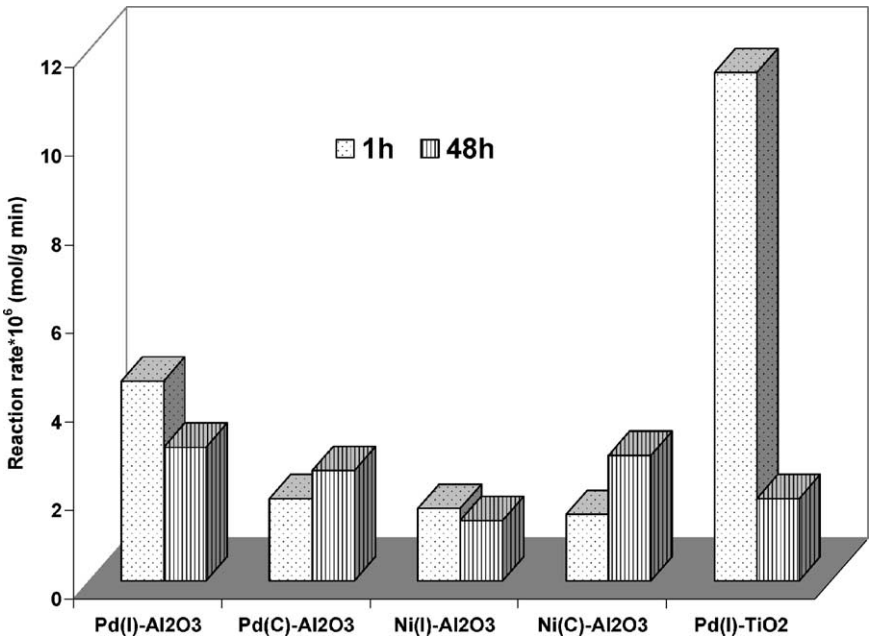

Fig. 4. The effect of pretreatment (1–3 h or 48 h) on initial DCM reaction rates at 200 °C, H_2/DCM ratio of 10 over selected catalyst samples.

sintering [34]. On the other hand, previous findings indicate that chlorine coverage under hydrodechlorination conditions decreases in the series Ru > Rh > Pd postulating that HCl formed on the Pd surface during DCM hydrodechlorination either desorbs to the gas phase or migrates to alumina [35]. Notwithstanding, the inhibition of palladium metal supported catalyst by the HX formed in the hydrodehalogenation of organic halides is generally accepted [36]. It can also be seen from Table 2 that spent Pd(I)–TiO_2 adsorbed less chlorine than spent Pd(I)–Al_2O_3 but, the former deactivated faster when exposed 48 h to a DCM stream at room temperature. The oxygen vacancies of titania are known to capture chloride species, so exposure to the chlorinated reactant appears to alter the nature of DCM and/or hydrogen activation step by altering the electronic structure of the adsorption site(s). Pd(I)–TiO_2 also deactivated after the first catalytic run. The BET surface area of a spent Pd(I)–TiO_2 sample decreased from 33 to 14 m^2/g and hydrogen chemisorption was inhibited after DCM hydrodechlorination reaction, vide infra. The latter result is in agreement with Dow and Huang who reported that reduction of the titania support is difficult when chorine atoms are incorporated into the oxygen vacancies of titania [37].

Table 2
Chloride contents of selected samples

Catalyst	Cl (wt.%)
Pd(I)–Al_2O_3 fresh	0.04
Pd(I)–Al_2O_3 after reaction[a]	0.8
Pd(I)–Al_2O_3[b]	3.9
Ni(I)–Al_2O_3[c]	2.4
Pd(I)–TiO_2 after reaction[d]	0.21

[a] Previously exposed 48 h to the reaction stream at 25 °C.
[b] Exposed 1–3 h to the reaction stream at 25 °C and 48 h at 200 °C.
[c] Exposed 1–3 h to the reaction stream at 25 °C and 36 h at 200 °C.
[d] Previously exposed 1–3 h to the reaction stream at 25 °C.

3.4. Hydrogen chemisorption and temperature-programmed reduction (TPR)

As a first approximation, hydrogen chemisorption uptakes, metal dispersions, particle sizes and TOF of selected Pd supported on Al_2O_3 and TiO_2 is provided in Table 3. Hydrogen chemisorption on Ni supported alumina and titania catalysts was below analytical detection limits (0.05 loops). Particle sizes of Pd loaded catalysts were estimated from metal dispersion using d_s (nm) = 112/D(%) assuming spherical particles [38]. The assignment of metal particle size/dispersion values based on chemisorption measurements is limited, since it assumes an exclusive H:Pd or H:Ni stoichiometry and ignores possible surface coverage effects and possible metal site blocking by residual halogen [39]. Nevertheless, diminished hydrogen chemisorption on Pd(I)–Al_2O_3 may be attributed to sintering of Pd particles. The same phenomenon was observed on Pd(I)–TiO_2 samples used (about 16 h), on a fresh Pd(I)–TiO_2 sample following pretreatment in air at 600 °C, and on fresh Pd(C)–TiO_2 catalysts. A strong inhibiting effect of hydrogen chemisorption is characteristic of strong metal–support interactions (SMSI) [40]. The suppression in hydrogen chemisorption has been ascribed to the physical blockage of metal particles by the mobile TiO_x phase, which is formed due to facile reduction of the TiO_2 in the presence of metal and hydrogen [40]. Initial TOFs increased with increasing particle size for catalysts pretreated using standard pretreatment (calcination in static air at 300 °C).

Table 3
Hydrogen chemisorption of selected Pd supported samples

Catalyst	H_2 chemisorption ($\mu mol/g_{cat}$)	Dispersion (%)	Particle size (nm) $D_{s,H2}$	Initial TOF (s^{-1})
Pd(C)–Al_2O_3	5.7	24.5	4.6	0.026
Pd(I)–Al_2O_3	4.3	18.1	6.2	0.083
Pd(I)–TiO_2	2.5	10.7	10.5	0.357
Pd(C)–TiO_2	0.005	<0.16[a]	–	–
Pd(I)–Al_2O_3[b]	0.2	1.1	102	[c]
Pd(I)–TiO_2[b]	–	<0.8[a]	–	[c]
Pd(I)–TiO_2[d]	0.4	1.6	70	0.106

[a] Lower than detection limit.
[b] After reaction.
[c] These used samples were not further tested in DCM hydrodechlorination.
[d] Pretreated in air under static conditions at 600 °C.

However, when Pd(I)–TiO_2 was calcined in air under static conditions at 600 °C particle size increased and TOF also decreased.

In order to obtain preliminary insights into the nature of the species involved in DCM hydrodechlorination H_2-TPR runs were performed over fresh palladium and nickel supported alumina and titania catalysts. The corresponding H_2-TPR profiles are shown in Figs. 5–8. The H_2-TPR profile of a Pd(C)–Al_2O_3 sample (trace (a), Fig. 5) shows a negative peak around 90 °C and a broad negative feature between 400 and 700 °C. The hydrogen evolution at 90 °C corresponds to decomposition of a palladium hydride phase formed at lower temperatures during TPR. The formation of Pd in this oxidized sample might be due to adsorption of CO or other organic fragments from the $Pd(acac)_2$ precursor onto the generated PdO. This result suggests that decomposition to PdO proceeded via the evolution of CO, CO_2 and a variety of CHO fragments. MS analysis confirms the existence of residual organics. The MS signals up to 100 amu indicate that mass 28 evolved around 550 °C together with hydrogen, likely due to decomposition of carbonaceous compounds sitting deep inside the porous alumina matrix. Interestingly, the negative broad feature disappeared after heating a Pd(C)–Al_2O_3 sample at 200 °C in O_2 for 1 h.

TPR of Pd(I)–Al_2O_3 (trace (b), Fig. 5) shows a hydrogen consumption peak at ca. 199 °C with a shoulder around 290 °C and a broad signal under the base line from 300 to

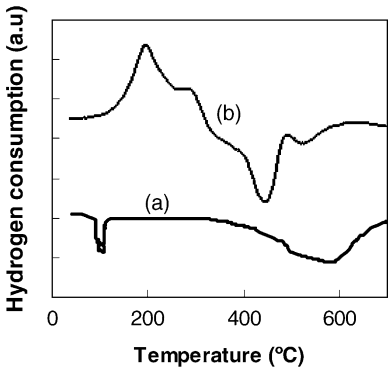

Fig. 5. H_2-TPR profile of Pd loaded xerogel γ-alumina catalysts: (a) Pd(C)–Al_2O_3; (b) Pd(I)–Al_2O_3.

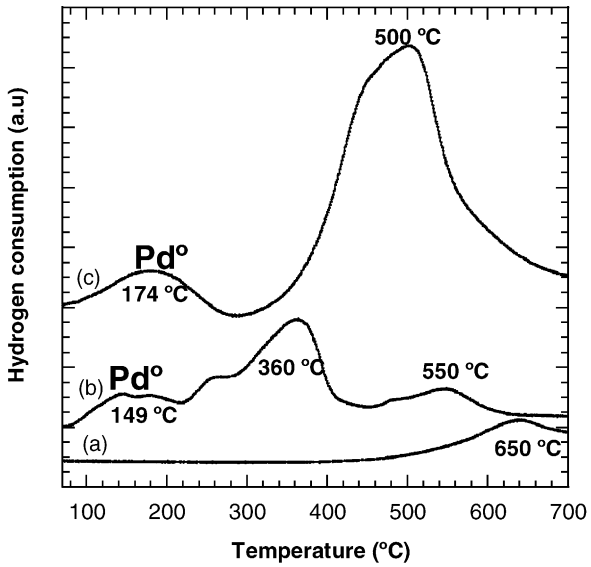

Fig. 6. H_2-TPR profile of Pd loaded xerogel titania catalysts: (a) TiO_2; (b) Pd(I)–TiO_2; (c) Pd(C)–TiO_2.

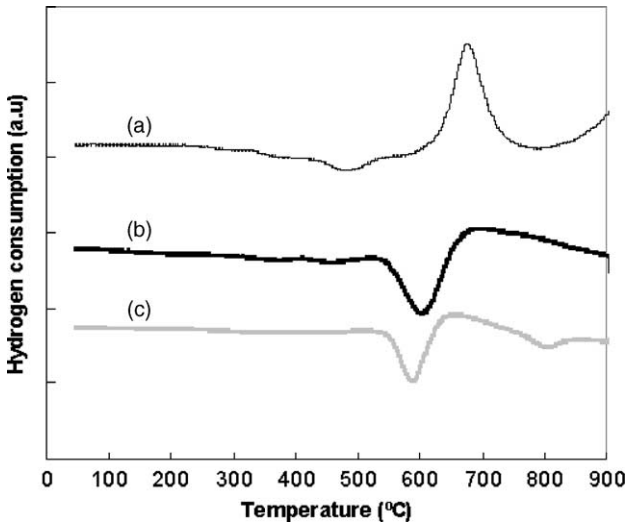

Fig. 7. H_2-TPR profile of Ni loaded xerogel γ-alumina catalysts: (a) Ni(C)–Al_2O_3; (b) Ni(I)–Al_2O_3; (c) Ni(I)–Al_2O_3 after DCM hydrodechlorination.

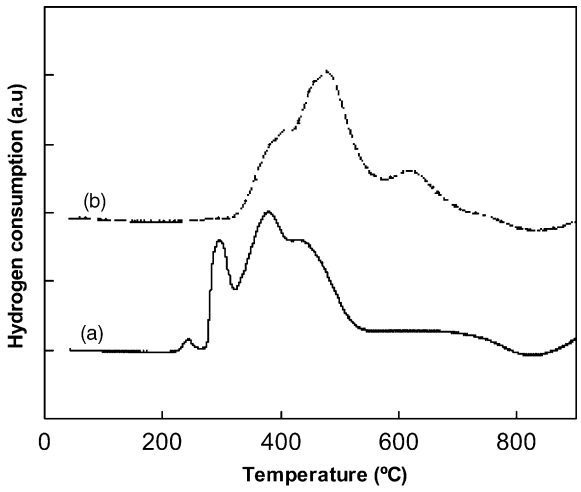

Fig. 8. H_2-TPR profile of Ni loaded xerogel titania catalysts: (a) Ni(I)–TiO_2; (b) Ni (C)–TiO_2.

500 °C with a minimum at 440 °C. The peak at 199 °C is assigned to bulk PdO reduction. MS analysis shows that together with the H_2 signal, a mass of 28 is also released around 290 °C. Again, different masses (18, 28, 43, 78, etc.) are evolved with hydrogen around 440 °C due to decomposition of organic residues. TPR experiments performed on blank xerogel alumina did not show any reducibility of the support in the 50–700 °C range indicating that organics used to synthesize the support were totally oxidized during support calcination.

Fig. 6 shows the characteristic H_2-TPR profiles of Pd supported titania samples treated in Ar at 130 °C. Traces (a), (b) and (c) correspond to TiO_2, Pd(I)–TiO_2 and Pd(C)–TiO_2, respectively. Commercial titania was found to be reduced at very high temperature (around 743 °C) and TPR profile is very broad, ranging from 550 to 774 °C [41]. Therefore, the peak at 650 °C in trace (a) is attributed to the partial reduction of the titania support. The TPR profile of Pd impregnated catalyst, trace (b), exhibits reduction peaks at 149, 260 (shoulder), 360 and 550 °C. The feature at 149 °C is assigned to the one-step reduction of bulk PdO. Hydrogen consumption at this temperature corresponds to reduction of about 53% of hydrogen necessary for reduction of PdO to metallic palladium. MS analysis shows that together with H_2 consumption at 260° C masses 28, 57, etc. evolved. The latter one is most likely due to acetone. Kohler et al. [42] proposed that metal acetylacetonates are partly decomposed by the catalytic action of the acidic and basic sites of the support involving the splitting of the acetylacetonate ligands and, possibly, the further transformation to acetone and acetic acid which strongly adsorb on the support. Arnoldy and Moulijn [43] showed that reduction of acetone required H_2 consumption and resulted in the production of CH_4. The reduction peak at 360 °C is likely due to a PdO surface phase that is interacting strongly with the support and corresponds to reduction of 83% of the Pd species in Pd(C)–TiO_2. The small broadened peak at 550 °C in trace (b) is attributed to the partial reduction of the titania support. The total hydrogen consumption corresponds to reduction of about five times the hydrogen necessary for reduction of loaded palladium confirming SMSI.

TPR of cogelled Pd(C)–TiO_2 sample (trace (c), Fig. 6) shows peaks at 174 and 500 °C. Peak at 174 °C is assigned to bulk PdO reduction. The large peak at 500° C is attributed to H_2 consumption of the titania carrier. The reduction of titania in Pd loaded titania samples is shifted to lower temperatures as compared to bare titania [44] and can be attributed to hydrogen dissociation at the surface of the Pd particles and the successive spillover of dissociated hydrogen atoms that can reduce TiO_2 more easily. Reduction at higher temperature give rise to SMSI between Ti^{3+} and Pd which could stabilize Ti^{3+}, i.e. titania is partly reduced and suboxide phase migrates onto the metal particles. Total hydrogen consumption corresponds to reduction of about nine times the hydrogen necessary to reduce loaded palladium. Since chemisorption uptake was inhibited on this sample it suggests that part of metal surface partially covered by TiO_x is blocked as has been reported [40].

The TPR patterns of fresh and used Ni(I)–Al_2O_3 and fresh Ni(C)–Al_2O_3 samples are shown in Fig. 7. The TPR profile of Ni(C)–Al_2O_3, (trace (a)), shows a negative peak around 480 °C indicative of hydrogen evolution and masses 12, 15, 18, 28, 42, 53, etc. as determined by MS. The hydrogen consumption peak around 680 °C revealed in the TPR of Ni(C)–Al_2O_3 is assigned to reduction of bulk NiO and corresponds to reduction of approximately 31% of Ni species. The relatively high reduction temperature compared with values obtained for unsupported NiO (382 °C) strongly points to the existence of interaction between Ni species and the alumina support. Li and Chen observed that at low content, nickel preferentially occupied the tetrahedral sites of alumina, forming a nonreducible surface spinel [45]. A negative peak around 600 °C is observed in the TPR profiles of fresh and used Ni(I)–Al_2O_3 samples (traces (b) and (c)). As previously reported [46] submitting $Ni(acac)_2/Al_2O_3$ catalysts to a previous heating at 250 °C in an oxidizing atmosphere ensured the decomposition of the acac ligands. However MS analysis indicates that together with hydrogen, masses 12, 14, 15, 28, 52, etc. are evolved around 600 °C due to decomposition of organic residues. No peaks due to reduction of Ni species are observed in these samples. The pseudo-peak at 680 °C does not correspond to H_2 consumption and no clear assignment can be given by MS. Decreased reducibility of nickel in NiO/Al_2O_3 catalysts has been observed and attributed to reinforced chemical interaction with the support, changes of the NiO crystallites size and incorporation of mobile Al^{3+} into NiO crystallites, and formation of non-stoichiometric or stoichiometric nickel aluminate [46].

TPR profiles of Ni(I)–TiO_2 and Ni(C)–TiO_2 samples are shown in Fig. 8. TPR of Ni(I)–TiO_2 sample (trace (a)) exhibits reduction peaks at 220, 300, 370 °C with a shoulder at 440 °C and a broad feature between 520 and 800 °C. The reduction of nickel oxide typically occurs around 320 °C on physical mixtures of NiO/TiO_2. Consequently, peaks below

400 °C (trace (a), Fig. 8) are assigned to reduction of NiO [47]. During reduction, two competitive processes are reported to occur, i.e. the reduction of NiO and interdifussion of NiO and TiO_2. At 300 °C the relative rate of reduction is high and a supported catalyst results, whereas at temperatures close to 500 °C considerable amounts of $NiTiO_3$ or a solid solution are formed [47]. Therefore, the shoulder observed at 440 °C in the TPR profile of a Ni(I)–TiO_2 sample might correspond to the reduction of a nickel titanate phase. At this temperature simultaneous CO evolution from decomposition of organic residues was also observed. Further reduction of $NiTiO_3$ causes segregation of the incorporated titanium ions and TiO_x islands on the surface of the nickel crystallites are formed [47]. The broad feature between 520 and 800 °C may be assigned to titanium ions transported to the surface of the nickel crystallites by a bulk diffusion mechanism. The total calculated hydrogen consumption is almost that required for reduction of Ni species. In the case of Ni(C)–TiO_2 samples, reduction peaks shifted to still higher temperatures (see trace b, Fig. 8). Geus and coworkers [47] observed that calcinations of Ni/TiO_2 catalysts at 750 °C resulted in the formation of $NiTiO_3$. The migratory TiO_x phase may have formed in Ni(C)–TiO_2 catalysts due to the reduction of $NiTiO_3$ which might have been produced during catalyst calcination at 700 °C. The total calculated hydrogen consumption amounts to twice the hydrogen necessary for the reduction of incorporated Ni, indicating reduction of the titania support and consequently SMSI.

Most authors agree that the thermolysis of supported complexes in an oxygen-containing atmosphere gives the corresponding metal oxides that are then reduced to generate dispersed metal particles [48–50]. Pd and Ni catalysts, synthesized in this work by impregnation, were calcined under static air at 300 or 350 °C, respectively, while cogelled catalysts were calcined at 700 °C. TPR of Pd or Ni supported on alumina and titania indicate that residual organics were present in all synthesized catalysts. The source of carbon in the Pd or Ni crystallites might mostly come from the palladium acetylacetonate precursor. Similar contamination of the Pd surface by carbon from palladium acetylacetonate was demonstrated by Vannice and coworkers in Pd/C and Pd/SiO_2 samples during a standard hydrogen reduction pretreatment at 300 °C [51]. TPR profiles in the present study indicate that the decomposition temperature of residual carbonaceous compounds under reducing conditions was higher for cogelled than for impregnated catalysts. Therefore, in cogelled samples residual organics appear to be located in the bulk, while they are more superficial in the impregnated catalysts, as expected from the preparation method used. Additionally, Pd(I)–Al_2O_3 appears to contain much more carbon residues than Pd(I)–TiO_2. Notwithstanding, low deactivation was observed in the former samples suggesting that carbon deposition is not a major factor in catalyst deactivation.

Interestingly, the size of metal particles in Pd(C)–Al_2O_3 is the smallest one, even though a high temperature (700 °C) was used to remove the organic ligands. This result suggests that Pd crystallites in Pd(C)–Al_2O_3 are less prone to sintering. As demonstrated by the textural analysis, this sample exhibits a monodisperse pore size distribution in the mesoporous domain, so it is reasonable to assume that palladium particles with a diameter of about 4.1 nm would be located inside porous alumina particles whose diameter is between 6.5 and 14 nm.

The role of the support in the hydrodehalogenation of organic halides has been studied by several authors [52–55]. For example, the effect of the support porous structure on the catalytic activity for hydrodechlorination of CFC-12 over Pd/Al_2O_3 was insignificant. However, it was found to influence the selectivity [52]. The structure sensitivity of the hydrodehalogenation reaction over Pd catalysts is still unclear. Although some authors have reported that the reaction is not structure sensitive [55], others have found that an increase in dispersion leads to a decrease in hydrodechlorination activity [9]. Our results indicate that the initial catalytic activity of catalysts pretreated in static air at 300 °C is inversely related to metal dispersion (%*D*). The initial observed TOF trend is: Pd(I)–TiO_2 > Pd(I)–Al_2O_3 > Pd(C)–Al_2O_3.Aramendía et al. [54], used catalysts having similar metal dispersions and showed that the acid–base properties of the support influence the specific activity of palladium supported catalysts in the liquid-phase hydrodechlorination of chlorobenzene. Basic supports such as ZrO_2 neutralized the HCl formed in the reaction. Our results do not show a clear trend of support acidity for DCM hydrodechlorination considering that the relative acidity of traditional supports decrease in the sequence: Al_2O_3 > TiO_2 > ZrO_2 > SiO_2. The accessibility of the metal function to the fluid phase appears to be a more important parameter, i.e. Pd impregnated over titania and alumina was much more active than cogelled Pd on the same supports. Furthermore, textural properties appear to be very important for DCM hydrodechlorination. For example, Ni–ZrO_2 which exhibits textural properties rather different than the other catalysts tested in this work is the less active catalyst for DCM hydrodechlorination.

4. Conclusions

This work allows us to draw several interesting conclusions as regards to the influence of the metal function, method of preparation and xerogel support on DCM hydrodechlorination:

- Overall, Pd loaded catalysts are more active and selective than those containing nickel and impregnated catalysts show superior activity than cogelled ones. However, cogelled alumina based catalysts appear to be more resistant to sintering and their activity increased after being exposed to the reaction mixture during 48 h.
- Pd(I)–TiO_2 exhibited the highest activity at 200 °C but, it was easily deactivated by the reaction mixture. Pd(I)–Al_2O_3 showed good activity and resistance to de-

activation up to about 48 h on stream, whereas Pd(I)–ZrO_2 and Pd(I)–SiO_2 showed moderate activity.

- Strong metal–support interactions (SMSI) were mainly observed in titania supported Pd and Ni catalysts. Under reducing conditions titania is partly reduced and part of metal surface may partially be covered by TiO_x. Also, the SMSI effect is observed in Ni loaded alumina catalysts, particularly those prepared by cogellation.

Acknowledgements

Financial support from Colciencias and Universidad de Antioquia through the project 1115-05-10129 is gratefully acknowledged. B.A. is grateful to red Vc from Cyted program and UdeA for supporting her stay in the group of professor Mario Montes.

References

[1] E.J. Shin, M.A. Keane, Appl. Catal. B 18 (1998) 241.
[2] USEPA, Needs for Eleven TRI Organic Chemical Groups, Pollution Prevention Research, Washington, DC, 1991.
[3] B. Coq, G. Ferrat, F. Figueras, J. Catal. 101 (1986) 434.
[4] D.I. Kim, D.T. Allen, Ind. Eng. Chem. Res. 36 (1997) 3019.
[5] L. Prati, M. Rossi, Appl. Catal. B 23 (1999) 135.
[6] M. Martino, R. Rosal, H. Sastre, F.V. Díez, Appl. Catal. B 20 (1999) 301.
[7] B.F. Hagh, D.T. Allen, Chem. Eng. Sci. 45 (1990) 2695.
[8] S. Ordoñez, F.V. Díez, H. Sastre, Appl. Catal. B 31 (2001) 113.
[9] W. Juszczyk, A. Malinowski, Z. Karpinski, Appl. Catal. A 166 (1998) 311.
[10] S. Ordoñez, F.V. Díez, H. Sastre, Ind. Eng. Chem. Res. 41 (2002) 505.
[11] B. Coq, J.M. Cognion, F. Figueras, D. Trournigant, J. Catal. 141 (1993) 21.
[12] D.J. Moon, M.J. Chung, K.Y. Park, S.I. Hong, Appl. Catal. A 168 (1998) 159.
[13] S.Y. Kim, H.C. Choi, O.B. Yanga, K.H. Lee, J. Chem. Soc. Chem. Commun. 21 (1995) 2169.
[14] B. Heinrichs, F. Noville, J-P. Pirard, J. Catal. 170 (1997) 366.
[15] I.H. Cho, S.B. Park, S.J. Cho, R. Ryoo, J. Catal. 173 (1998) 295.
[16] G. Sinquin, C. Petit, S. Libs, J.P. Hindermann, A. Kinnemann, Appl. Catal. B 27 (2000) 105.
[17] F. Mizukauni, US Patent 5,780,102 (1998).
[18] G. Pecchi, M. Morales, P. Reyes, React. Kinet. Catal. Lett. 61 (1997) 237.
[19] L.A. Contreras, J.L.R. Cerda, Actas do XVII Simposio Iberoamericano de Catálise, Porto, 2000, p. 205.
[20] A.F. Bedilo, K.J. Klabunde, J. Catal. 176 (1998) 448.
[21] E.P. Barret, L.G. Joiyner, P. Halenda, J. Am. Chem. Soc. 73 (1951) 373.
[22] B.C. Lippens, J.H. DeBoer, J. Catal. 4 (1965) 319O.
[23] E. López, S. Ordóñez, H. Sastre, F.V. Díez., J. Haz. Mater. B 97 (2003) 281.
[24] O. Levenspiel, Ingeniería de las Reacciones Químicas, Limusa Wiley, México, DF, 2004, p. 411.
[25] L.V. Azaroff, Elements of X-ray Crystallography, McGraw Hill, New York, 1968.
[26] M. Schneider, M. Wildberger, M. Maciejewski, D.G. Duff, T. Mallát, A. Baiker, J. Catal. 148 (1994) 625.
[27] L. Castro, P. Reyes, C. Montes de Correa, J. Sol. Gel. Sci. Technol. 25 (2002) 159.
[28] B.H. Aristizábal, Master Thesis, Chemical Sciences, UdeA, 2003, p. 141.
[29] G. Leofanti, M. Padovan, G. Tozzola, B. Venturelli, Catal. Today 41 (1998) 207.
[30] S. Ordóñez, F.V. Díez, H. Sastre, Communication in First European Congress in Chemical Engineering, Florence, 1997.
[31] A. Malinowski, D. Lomot, Z. Karpinski, Appl. Catal. B 9 (1998) 79.
[32] T. López, M. Morán, J. Navarrete, L. Herrera, R. Gómez, J. Non-Cryst. Solids 147 (1992) 773.
[33] Z.C. Zhang, B.C. Beard, Appl. Catal. A 188 (1999) 229.
[34] Y.H. Choi, W.Y. Lee, Catal. Lett. 67 (2000) 155.
[35] S. Ordoñez, F.V. Díez, H. Sastre, Appl. Catal. B 25 (2000) 49.
[36] F.J. Urbano, M.J. Marinas, J. Mol. Catal. A 173 (2001) 329.
[37] W. Dow, T. Huang, J. Catal. 160 (1996) 229.
[38] C. Belver, M.J. López-Muñoz, J.M. Coronado, J. Soria, Appl. Catal. B 46 (1996) 497.
[39] K.V. Murthy, P.M. Patterson, G. Jacobs, B.H. Davis, M.A. Keane, J. Catal. 223 (2004) 74.
[40] Y. Li, Y. Fan, H. Yang, B. Xu, L. Feng, M. Yang, Y. Chen, Chem. Phys. Lett. 372 (2003) 160.
[41] S.K. Maity, M.S. Rana, S.K. Bej, J. Ancheyta-Juárez, G. Murali Dhar, T.S.R. Prasada Rao, Appl. Catal. A 205 (2001) 215.
[42] S. Kohler, M. Reiche, C. Frobel, M. Baerns, Studies in Surface Science and Catalysis, vol. 91, Elsevier, Amsterdam, 1995, p. 1009.
[43] P. Arnoldy, J.A. Moulijn, J. Catal. 93 (1985) 38.
[44] W. Shen, M. Okumura, Y. Matsumura, M. Haruta, Appl. Catal. A 213 (2001) 225.
[45] C.H. Li, Y.W. Chen, Thermochim. Acta 256 (1995) 457.
[46] R. Molina, G. Poncelet, J. Catal. 173 (1998) 257.
[47] P.K. de Bokx, R.L.C. Bonne, J.W. Geus, Appl. Catal. 30 (1987) 33.
[48] J.C. Kenvin, M.G. White, M.B. Mitchell, Langmuir 7 (1991) 1198.
[49] M.G. White, Catal. Today 18 (1993) 73.
[50] R. Sekine, M. Kawai, K. Asakura, T. Hikita, M. Kundo, Surf. Sci. 278 (1992) 175.
[51] N. Krishnankutty, J. Li, M.A. Vannice, Appl. Catal. A 173 (1998) 137.
[52] W. Juszczyk, A. Malinowski, M. Bonarowska, Z. Karpinski, Polish J. Chem. 71 (1997) 1314.
[53] F.H. Ribeiro, C.A. Gerken, G.A. Somorjai, C.S. Kellner, G.W. Coulston, L.E. Manzer, L. Abrahams, J. Catal. 176 (1998) 352.
[54] M.A. Aramendía, V. Boráu, I.M. García, C. Jiménez, F. Lafont, A. Marinas, J.M. Marinas, F.J. Urbano, J. Catal. 187 (1999) 392.
[55] J.A. McCaulley, J. Phys. Chem. 97 (1993) 10372.